A Dynamic Model for the Interaction of Caustic Reagents with Acidic Oils

This paper describes the mechanisms and a quantative analysis of the interaction between a multicomponent acid mixture with a spectrum of caustic solutions. A physico-chemical model of the acidic oil/caustic system has been proposed which demonstrates the effect on dynamic interfacial tension (IFT) of variations in caustic concentration as well as changes in the initial composition and ionization properties of the constituent acids of the oleic phase. The model relies on the Langmuirian theory of interfacial sorption kinetics in addition to the Nernstian theory of convective diffusion. Pertinent kinetic and mass transfer parameters for all contributing surface-active species were determined from a recently proposed single-component dynamic model (Chiwetelu et al., 1988a). The validity of this multicomponent dynamic model was confirmed by the close agreement between predicted IFT and experimental data for a binary carboxylic acid system in contact with a broad range of caustic concentrations.

Chris I. Chiwetelu
Vladimir Hornof
Graham H. Neale
Chemical Engineering Department
University of Ottawa
Ottawa, Ontario, Canada K1N 6N5

Introduction

Typically, heavy oils have API gravities in the range of 10 to 25 while their viscosities at reservoir conditions may be as high as 1,000 mPa·s. When a heavy oil reservoir is waterflooded, most of the oil in place remains unrecovered due to the fact that the viscous floodwater fingers easily through the formation thereby stranding the oil. Further injection of water cannot mobilize the stranded oil because of relatively large capillary forces restraining the oil in the pores of the reservoir matrix. If the interfacial tension between the oil and the invading aqueous phase can be lowered to values near 1 mN/m or lower, the capillary forces may be overcome to the extent that the residual oil is mobilized and subsequently recovered.

Although Nutting (1927) and Subkow (1942) had suggested the addition of small amounts of alkaline reagents to the floodwater as a means of improving oil recovery, they did not give any rational explanation for the observed effectiveness of the alkalis. Lochte (1952) recognized that reactive species such as carboxylic acids and phenols must be present in the crude for the caustic flooding to be effective. Other investigators (Seifert and Teeter, 1970a,b; Jang et al., 1982) confirmed the presence of aliphatic, acylic and aromatic carboxylic acids in heavy oils. While the exact identity of these acids has not yet been fully established, their molecular weights generally lie in the range of 200–700. For the purpose of designing effective caustic systems for the recovery of heavy oils and bitumen from tar sands, we need to know not just the identity of the crude oil acids but also their original concentrations in the crude under reservoir conditions.

The precise mechanism for the reactions between caustic reagents with crude oil acids is still largely unclear. We do know that surface active soap species are formed *in situ* as a result of acid-base-like reactions occurring between the caustic agents present in the water with the acids of the oleic phase. When these surface active anions accumulate sufficiently at the oil/water interface, the IFT may be drastically lowered. Several researchers (Jennings, 1975; McCaffery, 1976; Trujillo, 1983; Babu et al., 1984) have observed the dynamic nature of the IFT which arises in caustic-acidic crude systems. The IFT has also been shown to vary with crude oil type, reservoir salinity, and the alkalinity of the floodwater.

In attempting to rationalize the complex reactions that occur at the oil-water interface between reactive species present in both fluids, it is reasonable to assume that the transient IFT would eventually attain an equilibrium value. We therefore need an appropriate equilibrium model as a first step in the development of the dynamic one. Patil et al. (1975) proposed a system chemistry for the interaction of caustic with fatty acids. Chan and Yen (1982) and Ramakrishnan and Wasan (1983) pro-

Correspondence concerning this paper should be addressed to G. H. Neale.

posed equilibrium models of the acidic crude/caustic system in which the crude oil acids were represented by one single species labeled 'HA'. Based on information currently available on the chemistry of crude oil acids, it is unlikely that a single species can adequately represent such a complex mixture. A realistic model must therefore take into account the entire range of surface active acids present in any given crude. Based on this philosophy, we have consistently used oleic phases of known composition in our effort to obtain relevant information on the interfacial behavior of single carboxylic acids contacted with a wide range of caustic concentrations. In a recent paper (Chiwetelu et al., 1988b), we proposed an equilibrium model of the acidic oil/caustic system. We showed that the pK_a of the acid largely governs the magnitude of the IFT for any given caustic concentration. Bansal et al. (1978) proposed that surface-inactive soap complexes are formed from reactions between excess sodium ions and the surface active soap anions. We found from our previous studies that the equilibrium constant governing the formation of this inactive soap complex is the other important parameter affecting interfacial tensions.

England and Berg (1971) were the first in recent times to apply a diffusive-kinetic analysis for describing surfactant transport between two semiinfinite and immiscible phases. Rubin and Radke (1980) extended the treatment of England and Berg to finite phases, while Trujillo (1983) used the former analysis in his study of dynamic IFT in crude oil/caustic systems. A recent model proposed by Borwankar and Wasan (1986) also attempted to account for the dynamic IFT of crude oil-caustic systems using sorption rate constants. Both Trujillo (1983) and Borwankar (1986) measured their dynamic IFT by means of the classical spinning drop tensiometer. While this technique is used widely for IFT measurements, there have been lingering doubts as to the accuracy of tension data obtained therefrom. Currie and van Nieuwkoop (1982) and Capelle (1981) showed that the IFT values determined from spinning drop tensiometry are influenced by buoyancy forces acting on the rotating oil droplet as well as the speed and duration of spinning. In the present investigation, we have used a novel technique called micropendography (Chiwetelu et al., 1988c) for the measurement of dynamic IFT. A rectangular micro cell (10 mm × 5 mm × 21 mm) made of optically flat glass normally holds about 1 mL of the aqueous phase. An upward pendant oil droplet (typically 1–5 mm in diameter) is then formed from a needle attached to a microsyringe but immersed in the aqueous phase. In micropendography, changes in the shape of the experimental droplet are recorded with a high-speed camera. Measurements of the linear dimensions of the droplet can then be made from photographic images, and the IFT is calculated by fitting a Laplacian curve (Chiwetelu et al., 1988c) through the measured coordinate points. This measurement technique was shown to give quite reliable and accurate tensions in the low to moderate regimes.

Recently, we proposed a single-component dynamic model (Chiwetelu et al., 1988a) which is a physico-chemical analysis applied to the specific geometry of the micropendographic measurement system. In this model, the powerful tool of nonlinear regression (Marquardt, 1963) was combined with sensitivity analysis (Bard, 1974) in order to obtain reliable estimates of the sorptive kinetic rate parameters that influence the dynamic interfacial tension. In this paper, we extend the dynamic analysis to the case of a defined multicomponent acidic oil contacted with a spectrum of aqueous caustic concentrations. Since we are essentially dealing with an electrically charged interface, we have used a geometrical model to delineate the zone where all interfacial reactions occur and where the electrical charge resides. Outside this zone, we have defined interfacial sublayers through which mass transfer from the bulk to the interface occurs (see Figure 1 in Chiwetelu et al., 1988b). This geometrical model also shows the diffusive and kinetic steps through which the acid species initially present in the oil is transported to the interface where it is partitioned to and ionizes at the aqueous sublayer. The surface-active soap anion is thus formed, and it gets adsorbed at the oil-water interface giving rise to an electrical double layer. The surface concentration of this soap anion is reduced by desorption to the aqueous phase, particularly by the formation of the inactive soap complex in the presence of excess sodium ions. Sharma et al. (1984) argued that in view of Marangoni-type interfacial disturbances, transport of reactants from the bulk to the interface is necessarily by convective diffusion. Thus, in using the simplified Nernstian convective diffusion theory (Levich, 1962), the boundary layer thickness is not affected by the electrical charge on the interface.

In order to develop the sorption kinetic expressions, we have used the Langmuirian fractional surface coverage theory in which the interfacial potential was calculated with the aid of Gouy-Chapman's model. We have assumed in this analysis that the composition of the acid mixture is known to the extent that all pertinent mass transfer and kinetic parameters for all contributing surface-active species can be determined from the single-component dynamic model. The goal of the multicomponent analysis is the prediction of the interfacial behavior of a given acid mixture contacted with a defined aqueous caustic concentration. To demonstrate the validity of the proposed model, we carried out dynamic tension measurements for binary mixtures of oleic and lauric acids contacting different concentrations. The agreement between the experimental and predicted IFT values was quite good over the entire range of mixture compositions and caustic concentrations. It is our view that this multicomponent model, complemented with the single-component and equilibrium models, can provide a more realistic insight into the complex problem of acidic crude/caustic interactions.

Model Development

Basic assumptions

Some rather basic assumptions have to be made in order to apply current theories in interfacial science to the modeling effort. These assumptions are justified for very low concentrations, which is often the case in practice when acidic crude oils contact low concentration aqueous caustic solutions:

- Surface coverage is limited to a monolayer.
- Ideal behavior exists for all interacting species in the bulk phases and the interface. (This implies that the concentrations of all surface-active species, both in the respective bulk phases and in the interface, are so dilute that steric and coulombic forces of repulsion between molecules of the different species are minimal.)
- Each acid species present in the mixture undergoes the various interfacial reactions that had been previously outlined (Chiwetelu et al., 1988a; Chiwetelu, 1988), without any interference from other acidic constituents.
- Transport and sorption kinetic rate parameters determined

from the single-component equilibrium and dynamic models will be valid for any given mixture constituent and its associated surface active species.

• In keeping with Nernstian convective diffusion theory, each acid in the mixture together with its associated surface-active species sets up unique diffusion boundary layers which are not influenced by those of the other mixture constituents.

Sorption kinetic rate equations

Following an approach similar to that presented in the single-component model (Chiwetelu et al., 1988a), we can write down the rate expressions for any given acid component i in accordance with Langmuirian sorption kinetics for the different reaction steps as follows:

a. Adsorptive Dissociation of Acid from the Oleic Sublayer

$$R_{(a,HX_{o,i})} = k_{HX_{o,i}}\left[C_{HX_{o,i,s}}(\Gamma_{max} - \Gamma) - \frac{\Gamma_i}{K_{HX_{o,i}}} C_{H^+} \exp - \left(\frac{\epsilon\psi_o}{kT}\right)\right] \quad (1)$$

The exponential term in Eq. 1 and in the other equations presented in items b–d arises from the difference between bulk or sublayer concentration and the interfacial concentration of the same species in accordance with Boltzmann relationships.

b. Adsorption of X_i^- from the Aqueous Sublayer

$$R_{(a,X_i^-)} = k_{X_i}\left[C_{X_{i,s}}\left(\frac{\epsilon\psi_o}{kT}\right)(\Gamma_{max} - \Gamma) - \frac{\Gamma_i}{K_{X_i}}\right] \quad (2)$$

c. Adsorption of $NaX_{o,i}$ from the Oleic Sublayer

$$R_{(a,NaX_{o,i})} = k_{NaX_i}\left[C_{NaX_{o,i,s}}(\Gamma_{max} - \Gamma) - \frac{\Gamma_i}{K_{NaX_{o,i}}} C_{Na^+} \exp - \left(\frac{\epsilon\psi_o}{kT}\right)\right] \quad (3)$$

d. Adsorption of $HX_{w,i}$ from the Aqueous Sublayer

$$R_{(a,HX_{w,i})} = k_{HX_{w,i}}\left[C_{HX_{w,i,s}}(\Gamma_{max} - \Gamma) - \frac{\Gamma_i}{K_{HX_{w,i}}} C_{H^+} \exp - \left(\frac{\epsilon\psi_o}{kT}\right)\right] \quad (4)$$

We can combine Eqs. 2 and 4 by using the α parameter proposed originally by Borwankar and Wasan (1986). The final expression then becomes

$$R_{(a,X_i^- + HX_{w,i})} = R_{(a,X_i^-)} \exp - \left(\frac{\epsilon\psi_o}{kT}\right)\left[1 + \frac{C_{H^+}}{K^D_{HX_i}}\right] = k_{X_i}\alpha_i\left[C_{X_{i,s}}(\Gamma_{max} - \Gamma) - \frac{\Gamma_i}{K_{X_i}} \exp - \left(\frac{\epsilon\psi_o}{kT}\right)\right] \quad (5)$$

Species bulk transport equations

Rubin and Radke (1980) proposed a generalized convective diffusion equation (using the argument originally put forward by Nernst and later refined by Levich) to account for mass transfer from the bulk to the sublayer as follows

$$\frac{V_i dC_i}{dt} = - \frac{A_s D_i}{\delta_i}(C_i - C_{i,s}) \quad (6)$$

The boundary layer thickness δ_i has a unique value depending on the nature of the diffusing species and the medium involved. Equation 6 can be expanded for each relevant species of the multicomponent system as follows

Transport of $HX_{o,i}$ from the Bulk to the Oleic Sublayer

$$V_o \frac{dC_{HX_{o,i}}}{dt} = - \frac{D_{HX_{o,i}} A_s}{\delta_{o,i}}[C_{HX_{o,i}} - C_{HX_{o,i,s}}] \quad (7)$$

Transport of $NaX_{o,i}$ from the Oleic Phase to the Sublayer

$$V_o \frac{dC_{NaX_{o,i}}}{dt} = - \frac{D_{NaX_{o,i}} A_s}{\delta_{o,i}}[C_{NaX_{o,i}} - C_{NaX_{o,i,s}}] \quad (8)$$

Transport of X_i^- to the Aqueous Sublayer

$$V_w \frac{dC_{X_i^-}}{dt} = - \frac{D_{X_i^-} A_s}{\delta_{w,i}}[C_{X_i^-} - C_{X_i^-,s}] \quad (9)$$

Transport of $HX_{w,i}$ from the Bulk Aqueous Phase to the Sublayer

$$V_w \frac{dC_{HX_{w,i}}}{dt} = - \frac{D_{HX_{w,i}} A_s}{\delta_{w,i}}[C_{HX_{w,i}} - C_{HX_{w,i,s}}] \quad (10)$$

Equations 9 and 10 are then combined using α_i, and the result becomes

$$V_w \alpha_i \frac{dC_{X_i^-}}{dt} = - \frac{D_{w,i} A_s \alpha_i}{\delta_{w,i}}[C_{X_i^-} - C_{X_{i,s}^-}] \quad (11)$$

Equations of the multicomponent model

In the single-component analysis, we showed that the condition that there is no net accumulation at the sublayers implies that the rates of adsorption/desorption of any given species by sorption kinetics must be equal to the diffusional flux of the same species. This identity makes it possible for the sublayer concentrations to be solved for explicitly. By substituting the expressions for the sublayer concentrations into the bulk transport equations, the diffusive-kinetic expressions are obtained as follows

For the species $HX_{o,i}$

$$V_o \frac{dC_{HX_{o,i}}}{dt} = - \frac{D_{HX_{o,i}} A_s k_{HX_{o,i}}}{[k_{HX_{o,i}}\delta_{o,i}(\Gamma_{max} - \Gamma) + D_{HX_{o,i}}]} \cdot \left[C_{HX_{o,i}}(\Gamma_{max} - \Gamma) - \frac{\Gamma_i}{K_{HX_{o,i}}} C_{H^+} \exp - \left(\frac{\epsilon\psi_o}{kT}\right)\right] \quad (12)$$

For the Species $NaX_{o,i}$

$$V_o \frac{dC_{NaX_{o,i}}}{dt} = -\frac{D_{NaX_{o,i}} A_s k_{NaX_{o,i}}}{[k_{NaX_{o,i}} \delta_{o,i}(\Gamma_{max} - \Gamma) + D_{NaX_{o,i}}]} \cdot [C_{NaX_{o,i}}(\Gamma_{max} - \Gamma)] + \frac{D_{NaX_{o,i}} A_s k_{NaX_{o,i}}}{[k_{NaX_{o,i}} \delta_{o,i}(\Gamma_{max} - \Gamma) + D_{NaX_{o,i}}]} \cdot \left[\frac{\Gamma_i}{K_{NaX_{o,i}}} C_{Na^+} \exp - \left(\frac{\epsilon\psi_o}{kT}\right)\right] \quad (13)$$

For the Combined Aqueous-Phase Species $(X^- + HX)_{w,i}$

$$V_w \frac{dC_{X_i}}{dt} = -\frac{D_{w,i} A_s k_{X_i}}{\left[k_{X_i} \delta_{w,i}(\Gamma_{max} - \Gamma) + D_{w,i} \exp - \left(\frac{\epsilon\psi_o}{kT}\right)\right]} \cdot \left[C_{X_i}(\Gamma_{max} - \Gamma) - \frac{\Gamma_i}{K_{X_i}} \exp - \left(\frac{\epsilon\psi_o}{kT}\right)\right] \quad (14)$$

For an Overall Species Mass Balance

$$\frac{d\Gamma_i}{dt} = \sum_{i=1}^{M} R_{(a,i,j)}, \; j = 1, 2 \quad (15)$$

The expansion of Eq. 15 leads to an expression for each individual Γ_i as follows

$$\frac{d\Gamma_i}{dt} = \frac{D_{HX_{o,i}} k_{HX_{o,i}}}{[k_{HX_{o,i}} \delta_{o,i}(\Gamma_{max} - \Gamma) + D_{HX_{o,i}}]} \cdot \left\{C_{HX_{o,i}}(\Gamma_{max} - \Gamma) - \frac{\Gamma_i}{K_{HX_{o,i}}} C_{H^+} \exp - \left(\frac{\epsilon\psi_o}{kT}\right)\right\} + \frac{D_{NaX_{o,i}} k_{NaX_{o,i}}}{[k_{NaX_{o,i}} \delta_{o,i}(\Gamma_{max} - \Gamma) + D_{NaX_{o,i}}]} \cdot \{C_{NaX_{o,i}}(\Gamma_{max} - \Gamma)\} - \frac{D_{NaX_{o,i}} k_{NaX_{o,i}}}{[k_{NaX_{o,i}} \delta_{o,i}(\Gamma_{max} - \Gamma) + D_{NaX_{o,i}}]} \cdot \left\{\frac{\Gamma_i}{K_{NaX_{o,i}}} C_{Na^+} \exp - \left(\frac{\epsilon\psi_o}{kT}\right)\right\} + \frac{D_{w,i} \alpha_i k_{X_i}}{\left[k_{X_i} \delta_{w,i}(\Gamma_{max} - \Gamma) + D_{w,i} \exp - \left(\frac{\epsilon\psi_o}{kT}\right)\right]} \cdot \left\{C_{X_i}(\Gamma_{max} - \Gamma) - \frac{\Gamma_i}{K_{X_i}} \exp - \left(\frac{\epsilon\psi_o}{kT}\right)\right\} \quad (16)$$

In addition to the above differential equations, the following four global algebraic relationships characterize the overall interfacial behavior of the multicomponent system as follows:

For the Overall Surfactant Surface Concentration Γ

$$\Gamma = \sum_{i=1}^{M_s} \Gamma_i \quad (17)$$

For the Surfactant Surface Concentration expressed in units of $\AA^2$ per Ion

$$A = \frac{1.6603 \times 10^{-8}}{\Gamma \times 10^{-4}} \quad (18)$$

For the Global Interfacial Potential ψ_o by the Gouy-Chapman Model

$$\psi_o = -51.4 \sinh^{-1}\left[\frac{136.9}{A\sqrt{C_{OH}}}\right] \quad (19)$$

For the Frumkin-Bolmer-Davies-Hachisu (FVDH) Equation of State Presented Earlier (Chiwetelu et al., 1988b) Giving the Prevailing Surface Pressure as a Function of Γ

$$\Pi = \gamma_o - \gamma = \frac{kT}{A_o} \ln\left(\frac{A}{A - A_o}\right) + \sqrt{\left(\frac{8D_c NC(kT)^3}{10^3 \epsilon^2}\right)}\left[\cosh\left(\frac{\epsilon\psi_o}{2kT}\right) - 1.0\right] \quad (20)$$

Solution of the Model Equations

We illustrate the general procedure for solving the model equations by examining a binary mixture of oleic and lauric acids dissolved in hexadecane. These two acids were also studied separately in the single-component experiments. If we have only a binary system, $M_s = 2$, thus eight diffusive-kinetic equations are needed in order that all relevant surface-active species of the mixture are considered. These equations are obtained simply by writing each of Eq. 12, 13, 14 and 16 twice (one each for each mixture component and its associated surface active species). Additionally, the four global relationships presented in Eq. 17–20 must be solved simultaneously with the eight differential equations at each time step. The solution of the different equations was carried out with the aid of the routine DGEAR (IMSL, 1984). Due to stiffness problems, the routine had to be supplied with the analytic Jacobian matrix of partial derivatives. This Jacobian matrix of partial derivatives was arrived at as follows. First, we identified the eight state variables of the system: $C_{HX_{o,oleic}}$, $C_{HX_{o,lauric}}$, $C_{NaX_{o,oleic}}$, $C_{NaX_{o,lauric}}$, $C_{X_{oleic}}$, $C_{X_{lauric}}$, Γ_{oleic}, and Γ_{lauric}. Next, we differentiated each of the eight differential equations with respect to each of the eight state variables resulting in 64 partial differential equations. It is important to recognize that Γ is a function of Γ_i and must be so treated in taking the partial derivatives. The size of the Jacobian matrix prohibits listing here, but they can be easily generated by applying the basic rules of differential calculus.

A computer program written for the purpose of solving the model equations starts by supplying the values of the relevant equilibrium and dynamic parameters which would have been determined from the single-component models. Initial values of all state variables are supplied as well as the initial time step size for solving the differential equations. Automatic adjustment of the step size is handled internally by the routine(DGEAR). Solutions to the model equations are obtained at any desired time interval, and the global value of Γ is calculated in accordance with Eq. 17. The corresponding surface pressure Π is

determined from Eq. 20. Subsequently, the dynamic interfacial tension for the system at the desired interfacial age can be easily determined once Π is known.

Experimental Method

Reagent grade oleic and lauric acids obtained from Fisher Scientific company were used as received. The hexadecane used as the oleic-phase solvent was a Fisher Certified reagent. Additional purification was effected by distilling the hexadecane under vacuum. Five different mixture compositions (see Table 1) were used for the study. Double-distilled, deionized and deaerated water was used to prepare the caustic solutions. All solutions used for the study were characterized by physical property measurements such as those listed in Table 1 for the binary mixtures. Data for some caustic solutions were reported previously (Chiwetelu et al., 1988c), while additional information may be found elsewhere (Chiwetelu, 1988). Dynamic IFT measurement was carried out by the use of photomicropendography in accordance with the procedure described previously (Chiwetelu et al., 1988c).

Results and Discussion

Interfacial Data

The density of the hexadecane used as the oleic-phase solvent was 770.1094 kg/m^3 at 25°C, and its viscosity under the same conditions was 3.0206 mPa · s. The physical property data of the mixtures given in Table 1 are not very different from the figures for the solvent given above. This suggests that the acid solutions were indeed sufficiently dilute to minimize the tendency to aggregate formation either in the oleic or aqueous phases (Tanford, 1980). As to the range of acid concentrations in the oleic phase, the limit of measurable IFT afforded by the micropendographic apparatus was the overriding constraint. Details of these limitations have been given elsewhere (Chiwetelu et al., 1988c). The decision to keep lauric acid concentration of the binary mixture constant, while varying that of oleic acid, arose from a careful evaluation of the results obtained from the single-component studies.

In order to appreciate the trends in the dynamic IFT data of these binary mixtures, plots such as those given in Figures 1–4 were prepared for all of the mixture systems. Figures 1–4 apply only to mixture M1 and the representative of the trends found for other mixture compositions. The data obtained with the mixture constituents on their own (from the single-component studies) were also plotted alongside those of the mixture as can be seen in Figures 1–4. In neutral water (pH 7.1), Figure 1 shows that the IFT of 0.10 mM oleic acid was about 40 mN/m and

Table 1. Mixture Composition and Physical Properties at 25°C

Code	Composition Lauric Acid in Hexadecane	Density kg/m^3	Viscosity mPa · s
M1	0.10 mM Oleic Acid + 0.02 M	770.6250	3.0293
M2	0.20 mM Oleic Acid + 0.02 M	770.6262	3.0306
M3	0.3125 mM Oleic Acid + 0.02 M	770.6308	3.0430
M4	0.6125 mM Oleic Acid + 0.02 M	770.6323	3.0443
M5	1.00 mM Oleic Acid + 0.02 M	770.6733	3.0472

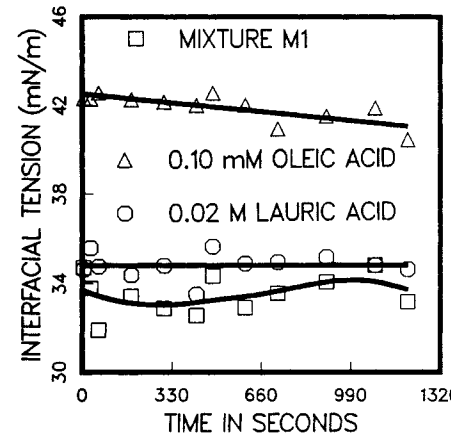

Figure 1. Dynamic IFT data for oleic acid and/or lauric acid solutions in hexadecane against water at pH of 7.1.

remained relatively unchanged even at interfacial ages above 20 minutes. The values for 0.02 M lauric acid were also little changed with contact time but these were much lower (about 35 mN/m). The tension values obtained with the binary mixture were identical with those of lauric acid. In Figure 2, the working NaOH concentration was 0.25 mM with a measured pH of 10.3 at 25°C. We find a gradual drop in IFT (from 41–35 mN/m) with increasing contact time for the case of 0.10 mM oleic acid. At the working lauric acid concentration of 20 mM, the IFT values remained largely unchanged from those found using neutral water. However, the mixture gave tension values which were very close to those obtained with lauric acid alone. Some appreciable scatter in the IFT values plotted in Figures 1–4 is evident. These tension values were average figures obtained from replicate experiments and at least two sets of droplet coordinate measurements. The precision found at low caustic concentrations and small contact times was generally better than 1%. However, at higher caustic concentrations and longer contact times, the precision was about 10% which gave an average precision for the

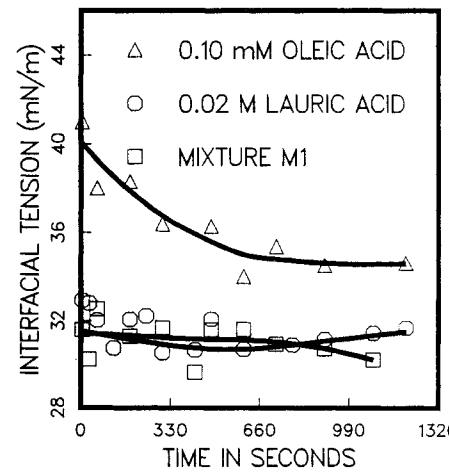

Figure 2. Dynamic IFT data for oleic acid and/or lauric acid solutions in hexadecane against aqueous 0.25 mM NaOH at pH of 10.3.

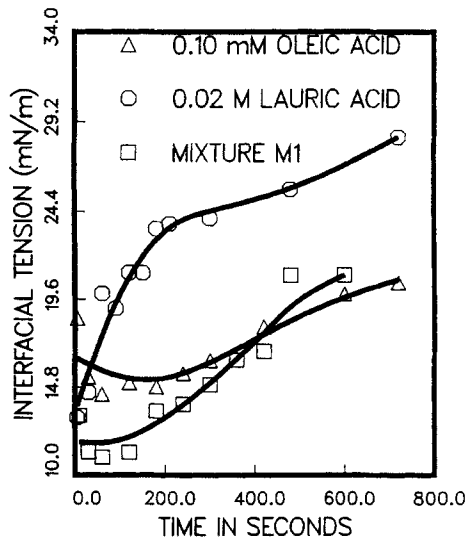

Figure 3. Dynamic IFT data for oleic acid and/or lauric acid solutions in hexadecane against aqueous 12.50 mM NaOH at pH of 12.1.

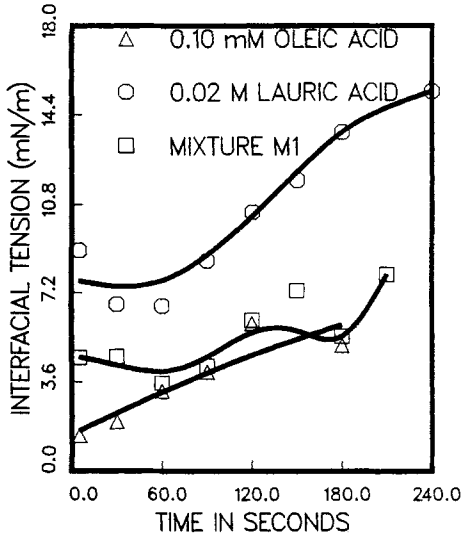

Figure 4. Dynamic IFT data for oleic acid and/or lauric acid solutions in hexadecane against aqueous 125.0 mM NaOH at pH of 13.0.

data of 5%. Trends in the dynamic IFT data obtained at caustic concentrations of 1.5 and 2.5 mM, respectively, were identical to those depicted in Figure 2. The acid mixture produced tension values which were quite similar to those of lauric acid alone. It is thus clear that lauric acid was the predominant species at low NaOH concentrations. From a previous study (Chiwetelu et al., 1988b), the pK_a value calculated for lauric acid was about 9, while the value for 0.10 mM oleic acid was about 6. However, as was also previously shown, oleic acid had a higher inactive soap equilibrium constant than lauric acid. A higher inactive soap equilibrium constant corresponds to a faster rate of removal of the active soap anions from the interface as can be seen in Figure 2. This explains the predominance of lauric acid at low caustic levels in the aqueous phase.

In Figure 3, the caustic concentration was raised to 12.50 mM and the solution had a pH of 12.6. The IFT values were generally lower in comparison to the values plotted in Figure 2. All tension values showed an increasing trend as contact time increased. However, oleic acid produced lower IFT values which compared favorably with the values found for the mixture. Clearly, oleic acid has replaced lauric acid as the dominant interfacial species. This is so despite the fact that the ratio of lauric acid to oleic acid in mixture M1 was 200 to 1. Again from our equilibrium study of these two acids, we found that the pK_a of lauric acid at caustic levels above 2.5 mM was about 11. Thus only a small amount of this acid actually ionized at higher caustic concentrations. The trend observed in Figure 3 was again manifested at a caustic level of 125 mM (pH of 13.0). The tension values for oleic acid moved even closer to those of the mixture. Similar trends were obtained with other mixture compositions such as M2–M5. Additional work is currently being undertaken with longer chain fatty acids in ternary mixtures in order to determine whether the qualitative trends of the binary systems would be manifested.

The implications of the results of these binary studies to caustic waterflooding of acidic oils are noteworthy. It is well known that the initial caustic content of an alkaline slug is gradually depreciated due to alkaline adsorption and retention in the reservoir matrix as well as by dilution with connate water. Thus, at the onset of the waterflood not too far from the injection well, the more interfacially active acids of the crude oil are activated and influence oil mobilization and subsequent recovery. However, towards the center of the reservoir where the slug would have been considerably denuded, the more abundant, but interfacially weaker acids, would establish at the interface, and they may thus influence oil recovery at the latter stages of the flood. Thus, both types of acids may indeed influence caustic waterflooding but at different time frames and with markedly different results. We expect that most of the residual oil would be

Table 2. Mass Transfer Parameters of the Binary System

Parameter	Symbol	Values for Oleic Acid	Values for Lauric Acid
Oil-side Nernstian Film Thickness	δ_o	2.60×10^{-10} m	2.80×10^{-10} m
Water-Side Nernstian Film Thickness	δ_w	2.60×10^{-9} m	2.80×10^{-9} m
Acid Diffusivity in Oil	D_{HX_o}	2.7×10^{-10} m^2/s	3.4×10^{-10} m^2/s
Salt Diffusivity in Oil	D_{NaX_o}	2.7×10^{-10} m^2/s	3.4×10^{-10} m^2/s
Acid Diffusivity in Water	D_{HX_w}	4.5×10^{-10} m^2/s	5.6×10^{-10} m^2/s

Table 3. Ionization and Kinetic Parameters of M1 and M5 Components

Parameter	Symbol	Values for 0.10 mM Oleic	Values for 1.00 mM Oleic	Values for 0.02 M Lauric
Saturation Adsorption	Γ_{max}	5.5×10^{-6} mol/m^2	5.5×10^{-6} mol/m^2	3.7×10^{-6} mol/m^2
Acid Sorptive Equilibrium Constant	K_{HX_o}	1.8×10^{-4}	5.0×10^{-5}	5.3×10^{-7} (for NaOH < 2.50 mM) 2.6×10^{-8} (for NaOH > 2.50 mM)
Anion Sorptive Equilibrium Constant	K_X	4.4×10^6 m^3/mol	4.4×10^6 m^3/mol	7.1×10^3 m^3/mol
Salt Sorptive Equilibrium Constant	K_{NaX_o}	2.9×10^5	4.1×10^6	1.4×10^3
Acid Adsorption Rate Constant	k_{HX}	0.23 m^3/mol · s	0.23 m^3/mol · s	0.24 m^3/mol · s (for NaOH < 12.5 mM) 0.50 m^3/mol · s (for NaOH > 12.5 mM)
Salt Desorption Rate Constant	k_{NaX}	0.22 m^3/mol · s	0.22 m^3/mol · s	0.26 m^3/mol · s (for NaOH < 12.5 mM) 0.17 m^3/mol · s (for NaOH > 12.5 mM)
Anion Desorption Rate Constant	k_X	0.28 m^3/mol · s	0.28 m^3/mol · s	0.28 m^3/mol · s

produced early in the life of the project, if the caustic slug is well formulated and if propagation through the reservoir occurs without severe channeling or excessive caustic losses.

Model predictions

Before examining the tension values predicted by the model, it is instructive to examine briefly the parameter values. Independent variables such as initial acid and caustic concentrations, interfacial areas, and phase volumes were determined experimentally. Mass transfer variables calculated for each surface-active species are listed in Table 2. The procedure used in calculating these variables was described in detail elsewhere (Chiwetelu et al., 1988a; Chiwetelu, 1988). The Nernstian film thicknesses given in the table are quite small, but that too is a reflection of the low viscosity of the working solutions. In a separate parametric study, the film thicknesses were increased by about 300%, but we failed to detect any appreciable influence on the model predictions.

The ionization and kinetic parameters that most influence IFT are listed in Table 3 for mixtures M1 and M5, respectively. It was shown in the single-component dynamic model that the sorptive equilibrium constants, K_{HX_o} and K_{NaX_o}, were directly proportional to the acid ionization constant and the inactive soap dissociation constant, respectively. The sorptive kinetic rate constants appearing in Table 3 were similarly evaluated from the single-component analysis. The effects of varying acid and caustic concentrations on these parameters can be seen by a close examination of the data presented in Table 3.

Comparative plots of predicted and experimental dynamic IFT for mixture M5 are presented in Figures 5–8. Similar plots for other mixture systems were also prepared (Chiwetelu, 1988). At a caustic concentration of 0.25 mM (Figure 5), we find perfect agreement between model predictions and the experimental IFT values. In Figure 6, the NaOH level in the aqueous phase was 1.25 mM and again there is good agreement between the experimental and predicted tension values. When the caustic concentration was increased to 2.50 mM, there is some disparity between the model predictions and the experimental data. In this case, the experimental values were slightly higher as can be seen in Figure 7. Additionally, the predicted tension values were somewhat oscillatory and leveled out much sooner than the experimental data indicated. A similar discrepancy was found even in the single-component analysis. The

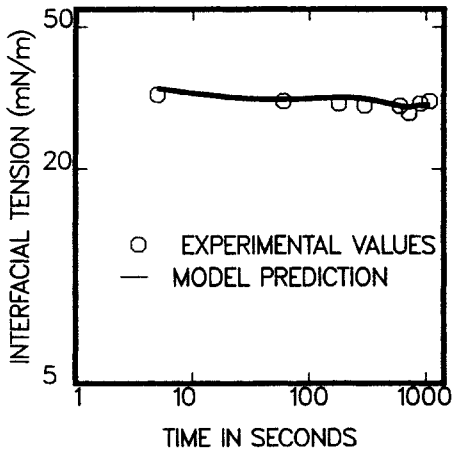

Figure 5. Experimental vs. predicted dynamic IFT behavior for Mixture M5 against aqueous 0.25 mM NaOH at pH of 10.3.

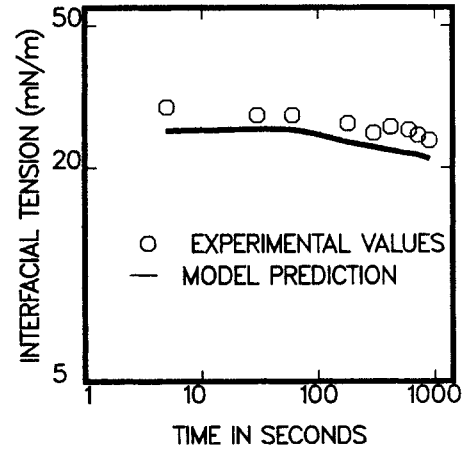

Figure 6. Experimental vs. predicted dynamic IFT behavior for Mixture M5 against aqueous 1.25 mM NaOH at pH of 11.1.

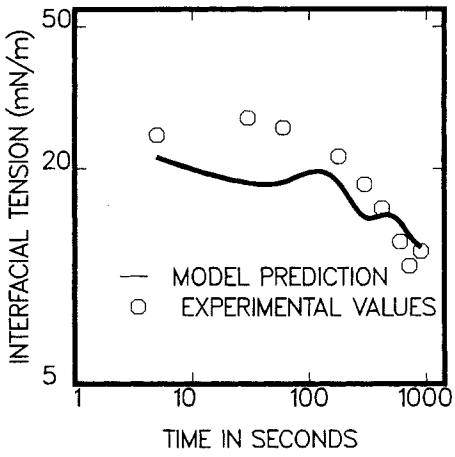

Figure 7. Experimental vs. predicted dynamic IFT behavior for Mixture M5 against aqueous 2.50 mM NaOH at pH of 11.4.

oscillatory nature of predicted tension data arose from the much shorter time steps which were used for solving the differential equations, particularly for the highly alkaline systems. Initial IFT values were often low, and they tended to increase at a faster rate thus necessitating the use of very small time steps. Its effect on the numerical solution of the differential equations was to increase the truncation error, and it became more apparent at longer contact times. In Figure 8, the agreement between model prediction and experimental data was good up to a contact time of 100 seconds. Thereafter, the models predicted nearly constant IFT values, while the experimental values continued to increase marginally. We showed in a previous publication (Chiwetelu et al., 1988c) that the accuracy of tension data obtained by micropendography at lower tension values and long contact times was reduced due to hydrodynamic instabilities associated with small pendant drops. In general, the agreement between the model predictions and the experimental IFT values was satisfactory for the entire range of mixture compositions, caustic concentrations, and interfacial contact times.

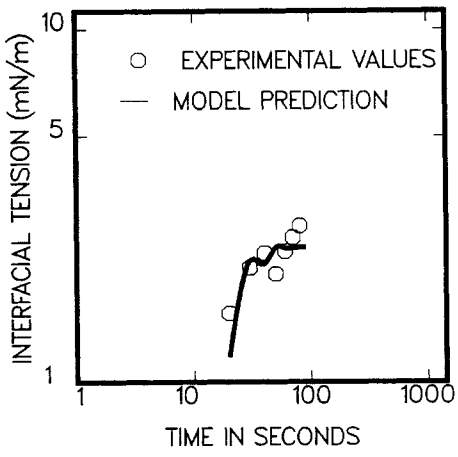

Figure 8. Experimental vs. predicted dynamic IFT behavior for Mixture M5 against aqueous 25.0 mM NaOH at pH of 12.3.

Concluding Remarks

- A physico-chemical model has been proposed to account for the dynamic IFT behavior in multicomponent acidified oleic systems contacted with a spectrum of aqueous caustic concentrations.
- This multicomponent model will predict the dynamic interfacial tension behavior of a known acid mixture exposed to varying aqueous NaOH solutions from the interfacial characteristics of the constituent acids.
- Data from binary mixture experiments showed that the more abundant lauric acid species were dominant at the interface at low caustic concentrations in the aqueous phase. However, at higher caustic levels, the less abundant, but interfacially more active, oleic acid became predominant.
- The dynamic IFT predicted by the model agreed reasonably well with the experimental data over a wide range of mixture compositions and NaOH concentrations.

Acknowledgment

The authors are grateful to the Natural Sciences and Engineering Research Council of Canada (NSERCC) for continuing support of their work.

Notation

A = surface area per molecule, Å^2
A_o = minimum surface area per molecule, Å^2
A_s = surface area, m^2
c, C = molar concentrations
D_c = dielectric constant of water
D_i = diffusion coefficient, m^2/s
HD = hexadecane
k = Boltzmann constant
k_i = sorptive rate constants
K_a = acid dissociation constant
K_D = salt distribution ratio water/oil
K_i = sorptive equilibrium constants
M = number of reactive species associated with a given acid
M_s = total number of components in the mixture
N = Avogadro number
R = universal gas constant
$R_{(a,i)}$ = net rate of adsorption/desorption of species, i
t = time
T = temperature, K
V = phase volume, droplet volume

Greek letters

α = association parameter
δ = Nernstian film thickness
ϵ = electronic charge
γ = interfacial tension, mN/m
Γ = surface concentration of adsorbed species
Γ_{max} = saturation adsorption, mol/m^2
ψ_G = the Gouy surface potential, mV
ψ_o = interfacial potential, mV
Π = surface pressure, mN/m
ρ = density
σ = surface charge density

Subscripts

HC = hydrocarbon
HX = acid species
i = phase identity, mixture constituents
j = number of phases
NaX = inactive soap species or salt
o = initial state, oleic phase
s = sublayer, steric

w, W = water, aqueous phase
x, X = anion, surfactant

Literature Cited

Babu, D. R., V. Hornof, and G. Neale, "Effects of Temperature and Time on Interfacial Tension Behaviour between Heavy Oils and Alkaline Solutions," *Can. J. Chem. Eng.*, **62**, 156 (1984).

Bansal, V. K., K. S. Chan, R. McCallough, and D. O. Shah, "The Effect of Caustic Concentration on Interfacial Charge, Interfacial Tension and Droplet Size: a Simple Test for Optimum Caustic Concentration for Crude Oils," *J. Can. Pet. Tech.*, **17**, 69 (1978).

Bard, J., "Nonlinear Parameter Estimation, Academic Press, 1974. Borwankar, R. P. and Wasan, D. T.: Dynamic Interfacial Tensions in Acidic Crude/Caustic Systems: I. A Chemical Diffusion-Kinetic Model," *AIChE J.*, **32**, 455 (1986).

Capelle, A., Measurement of Low Interfacial Tension between Crude Oil and Formation Water with Dissolved Surfactant by the Spinning Drop Technique: Fact or Fiction? in *Surface Phenomena in Enhanced Oil Recovery*, D. O. Shah, ed. Plenum Press, New York (1981).

Chan, M. and T. F. Yen, "A Chemical Equilibrium Model for Interfacial Activity of Crude Oil in Aqueous Alkaline Solution: The Effects of pH, Alkali and Salt," *Can. J. Chem. Eng.*, **60**, 305 (1982).

Chiwetelu, C. I., "Dynamic Interfacial Tension of Finite Reactive Systems Related to Enhanced Oil Recovery," PhD Thesis, University of Ottawa (1988).

Chiwetelu, C., V. Hornof, and G. H. Neale, "Mechanism for the Interfacial Reaction between Acidic Oils and Alkaline Reagents," *Chem. Eng. Sci.* (in press) (1988a).

——, "Interaction of Aqueous Caustic with Acidic Oils," *J. Can. Pet. Tech.*, **28**(4), 71 (1988b).

———, "The Measurement of Dynamic Interfacial Tension by Photomicropendography," *J. Coll. Interf. Sci.*, **125**, 586 (1988c).

Currie, P. K., and J. van Nieuwkoop, "Buoyancy Effects in the Spinning Drop Interfacial Tensiometer," *J. Coll. Interf. Sci.*, **87**, 301 (1982).

England, D. C., and J. C. Berg, "Transfer of Surface-Active Agents across a Liquid-Liquid Interface," *AIChE J.*, **17**, 313 (1971).

IMSL Corporation, *The IMSL Libraries: Problem-Solving Software Systems for Numerical Fortran Programming*, IMSL, Houston (Nov., 1984).

Jang, L. K., Y. I. Chang, M. Chan, and T. F. Yen, "Correlation of Petroleum Component Properties for Caustic Flooding," *AIChE Symp. Ser.*, **78**(212), 97 (1982).

Jennings, Jr., H. Y. "A Study of Caustic Solution—Crude Oil Interfacial Tensions," *Soc. Pet. Eng. J.*, **15**, 197 (1975).

Levich, V. G., *Physico-chemical Hydrodynamics*, Prentice-Hall, Englewood Cliffs, NJ (1962).

Lochte, H. L., "Petroleum Acids and Bases," *Ind Eng. Chem.*, **44**, 2597 (1952).

McCaffery, F. G., "Interfacial Tensions and Aging Behaviour of some Crude Oils against Caustic Solutions," *J. Can. Pet. Tech.*, **15**, 71 (1976).

Marquardt, D. W., "An Algorithm for Least Squares Estimation of Nonlinear Parameters," *J. Soc. Ind. Appl. Math.*, **11**, 431 (1963).

Nutting, P. G., "Principles Underlying Soda Process," *Oil and Gas J.*, **25**(50), 32, 106 (1927).

Patil, G. S., R. H. Mathews, and D. G. Cornwall, "Estimation of Ionization in Unstable Fatty Acid Monolayers from Desorption Kinetics," *Monolayers-Advances in Chemistry*, Ser. 144, E. D. Goddard, ed., ACS, Washington, DC, 44 (1975).

Ramakrishnan, T. S., and D. T. Wasan, "A Model for Interfacial Activity of Acidic Crude Oil/Caustic Systems for Alkaline Flooding," *Soc. Pet. Eng. J.*, **23**, 602 (1983).

Rubin, E., and C. J. Radke, "Dynamic Interfacial Tension Minima in Finite Systems," *Chem. Eng. Sci.*, **35**, 1129 (1980).

Seifert, W. K., and R. M. Teeter, "Identification of Polycyclic Naphthenic, Mono- and Di-Aromatic Crude Oil Carboxylic Acids," *Anal. Chem.*, **42**, 180 (1970a).

Seifert, W. K., and R. M. Teeter, "Identification of Polycyclic Aromatic and Heterocyclic Crude Oil Carboxylic Acids," *Anal. Chem.*, **42**, 750 (1970b).

Sharma, M. M., L. K. Jang, and T. F. Yen, "Transient Interfacial Tension Behaviour of Crude Oil-Caustic Interfaces," *SPE Res. Eng.*, **4**, 288 (1989).

Subkow, P., "Process for the Removal of Bitumen from Bituminous Deposits," U.S. Patent No. 2,288,857 (July, 1942).

Tanford, C., *The Hydrophobic Effect: Formation of Micelles and Biological Membranes*, Wiley, New York (1980).

Trujillo, E. M., "The Static and Dynamic Interfacial Tensions between Crude Oils and Caustic Solutions, *Soc. Pet. Eng. J.*, **23**, 645 (1983).

Manuscript received June 23, 1989, and revision received Nov. 22, 1989.